Available online at www.sciencedirect.com
ScienceDirect
Trans. Nonferrous Met. Soc. China 22(2012) 2131−2138
Transactions of Nonferrous Metals Society of China
www.tnmsc.cn

Banding structure formation during directional solidification of Pb−Bi peritectic alloys

HU Xiao-wu[1], LI Shuang-ming[2], AI Fan-rong[1], YAN Hong[1]

1. School of Mechanical-Electrical Engineering, Nanchang University, Nanchang 330031, China;
2. State Key Laboratory of Solidification Processing, Northwestern Polytechnical University, Xi'an 710072, China

Received 7 September 2011; accepted 1 April 2012

Abstract: Directional solidification experiments on Pb−Bi peritectic alloys were carried out at very low growth rate (v=0.5 μm/s) and high temperature gradient (G=35 K/mm) in an improved Bridgman furnace. The banding structures were observed in both hypoperitectic and hyperperitectic compositions (Pb−xBi, x=26%, 28%, 30% and 34%). Tree-like primary α phase in the center of the sample surrounded by the peritectic β phase matrix was also observed, resulting from the melt convection. The banding microstructure, however, is found to be transient after the tree-like structure and only the peritectic phase forms after a few bands. Composition variations in the banding structure are measured to determine the nucleation undercooling for both α and β phases. In a finite length sample, convection is shown to lead only to the transient formation of bands. In this transient banding regime, only a few bands with a variable width are formed, and this transient banding process can occur over a wide range of compositions inside the two-phase peritectic region.

Key words: directional solidification; segregation; Bridgman technique; Pb−Bi alloys; banding structure

1 Introduction

Several directional solidification studies in peritectic systems have reported the formation of banding microstructure in which primary α phase and peritectic β phase appear as bands [1−5]. TRIVEDI [6] has proposed a simple model of banding in peritectic systems that pertains to a high G/v ratio (G is the temperature gradient and v is the growth rate) regime, where both phases grow with a planar interface. This model predicts that under purely diffusion-controlled growth, α and β bands should form across the entire sample with widths λ_α and λ_β, which are constant and determined by the nucleation undercoolings Δt_n^α and Δt_n^β. Furthermore, it predicts that banding should only occur within the relatively narrow composition range Δc_0.

While in some systems, including Sn−Cd [7−10], Sn−Sb [11] and Zn−Cu [11], bands tend to form more or less uniformly along the entire sample at a high G/v ratio. In others like Pb−Bi, banding is originally found to be not easily reproducible or to be absent [12]. A more systematic study, shows that banding in this system is essentially transient and characterized by the formation of a few bands subsequent to the initial transient primary α phase. Moreover, it is found that band formation occurs over a much wider range of compositions that spans almost the entire two phase peritectic region comprised between c_α (composition of α at peritectic temperature) and c_β (composition of β at peritectic temperature). TRIVEDI [6] analyzed the limit of complete mixing in the melt and argued on the basis of the Scheil equation that convection should completely suppress the formation of bands in this limit. However, a quantitative model that treats band formation under the combined effects of diffusion and convection without complete mixing, which can account for the transient formation of bands, has remained lack. Furthermore, there has not yet been any direct quantitative test of the conceptual banding mechanism, either in a purely diffusive or in a combined diffusive/convective regime. At present, it is still unclear that this cycle is actually representative of how banding takes place, since the

Foundation item: Project (20110491492) supported by the China Postdoctoral Science Foundation; Project (20114BAB216017) supported by the Natural Science Foundation of Jiangxi Province, China; Project (GJJ12035) supported by the Science Foundation of the Educational Department of Jiangxi Province, China

Corresponding author: HU Xiao-wu; Tel: +86-791-3969633; Fax: +86-791-3969633; E-mail: xwhmaterials@yahoo.cn

DOI: 10.1016/S1003-6326(11)61439-8

analysis of solidified samples has not provided a direct picture of the way in which bands are formed so far.

The aim of this study is to quantitatively investigate the effect of composition on the microstructure formation in the Pb−Bi system, with the focus on the formation of transient banding, banding window and initial α phase growth. Quantitative analysis of this transient banding process and macrosegregation in initial α phase growth are carried out to establish the physics that destabilizes the sustained banding process under convective growth conditions.

2 Experimental

Pb−xBi (x=26%, 28%, 30% and 34%, mass fraction) alloys were made from Pb (99.99%) and Bi (99.99%) in an Ar atmosphere. According to the phase diagram [13], the Pb−26%Bi and Pb−28%Bi alloys have the hypoperitectic composition, while the Pb−30%Bi and Pb−34%Bi alloys have the hyperperitectic composition. The as-cast rods with dimensions of d1.7 mm × 100 mm were cut from the master ingot by electro-discharge machining. The specimen was inserted into an alumina tube which was prepared for directionally solidification (DS). DS experiments were carried out in an improved Bridgman vertical vacuum furnace which was described elsewhere [14,15]. During the DS processing, the furnace was heated to approximately 375 °C under a vacuum of 10^{-1} Pa with high purity argon to prevent the evaporation of the components in the Pb−Bi alloys. Samples were directionally solidified for a minimum length of 60 mm to ensure that several centimeters of growth beyond the initial transient were obtained before the interface was quenched. The temperature gradient was maintained at G=35 K/mm, and the growth velocity was selected to be v=0.5 μm/s. This velocity was selected to allow a planar solid-liquid interface for α and β phases with the present temperature gradient.

The longitudinal sections of the specimens were cut, mounted and polished. After polishing, the samples were etched with the reagent of 100 mL distilled water (H_2O), 10 mL nitric acid (HNO_3) and 4 g ammonium molybdate ($(NH_4)_6MO_7O_{24}\cdot 4H_2O$). An Olympus TG−3 optical microscope was employed to observe the microstructures of the specimens and an electro probe microanalysis (EPMA) was adopted to measure the concentration.

3 Results and discussion

3.1 Observation of banding structures

The present study confirmed the formation of the banding structure for the hypoperitectic and hyperperitectic compositions of Pb−Bi system. In previous studies [12,16,17], the directionally solidified microstructures under planar growth condition for the Pb−Bi peritectic alloys had some layers in the transition region from the initial α phase to β phase. The banding structures observed for four different compositions are shown in Fig. 1. The formation of bands after the initial first α phase formation shows some main characteristics.

1) For all the compositions studied, only a finite number of bands are formed, after which the rest of the samples are solidified as β phase. Therefore, banding is only transient.

2) The widths of the individual bands λ_α and λ_β, and the total band spacing $\lambda=\lambda_\alpha+\lambda_\beta$ vary with the solidified distance along the sample for the Pb−28%Bi alloy, as shown in Fig. 2. As can be seen, λ_α decreases with increasing distance along the sample, while λ_α increases.

3) For each composition, it is clearly seen in Fig. 1 that the β phase is prior to nucleate at the trijunction of α-liquid-crucible.

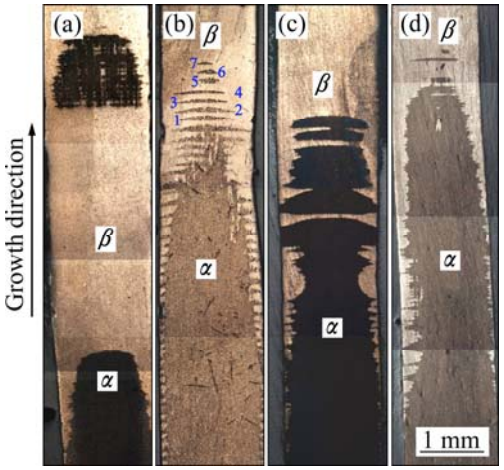

Fig. 1 OM images showing longitudinal microstructures of directionally solidified Pb−Bi alloys: (a) Pb−26%Bi; (b) Pb−28%Bi; (c) Pb−30%Bi; (d) Pb−34%Bi

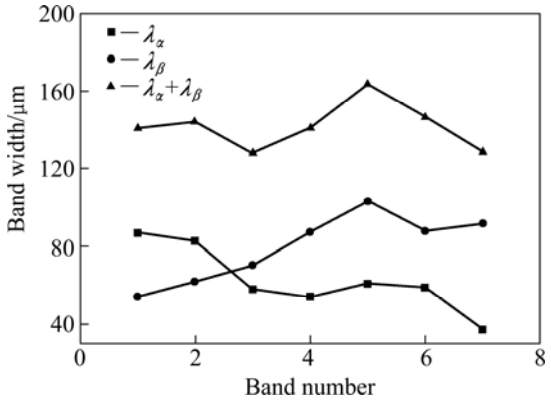

Fig. 2 Measured widths of α and β bands and total band spacing as function of band number for Pb−28% Bi alloy

3.2 Effect of composition on microstructure

Figure 3 shows the characterized lengths of banding structure observed in the present study, where the parameters of l_S, l_α^1 and l_α^2 can be defined as follows: l_S is the total length of the solidified sample, l_α^1 is the distance between the first peritectic β phase nucleation site and initial position and l_α^2 is the solidification distance for the disappearance of the initial primary α phase.

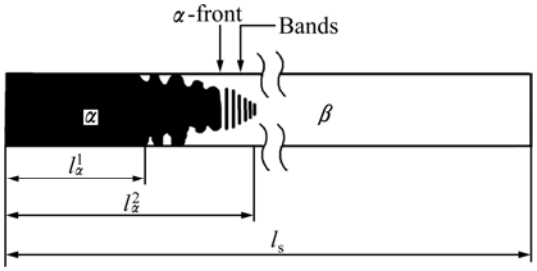

Fig. 3 Schematic drawing of oscillatory, banding structure and characterized length

The effect of composition on the formation of the banding structure was examined. Similar microstructures were observed, and some detailed comparisons, including the characterized lengths among four alloys with different compositions are listed in Table 1. The value of $l_\alpha^2 - l_\alpha^1$ presents the length of two phases growth region and f_α^1 is the solidified fraction of initial primary α phase before the nucleation of peritectic β phase at the S/L interface. It is obviously seen that l_α^1 decreases with an increase of Bi in composition. That indicates that the β phase forms at a lower solidification fraction since the composition at which β phase forms is reached at a smaller solidification fraction, as shown in Fig. 4. Additionally, the length of the two phase region decreases with increasing the solute composition.

Table 1 Characterized length of directionally solidified Pb−xBi alloys at low velocity

x	l_S/mm	l_α^1/mm	l_α^2/mm	$(l_\alpha^2-l_\alpha^1)$/mm	f_α^1
26%	70	36	45	9	0.51
28%	70	32	38	6	0.46
30%	70	28.5	33.5	5	0.41
34%	70	6	10.5	4.5	0.09

3.3 Concentration distribution in banding structure

A single transition from α phase to β phase in Pb−26%Bi alloy and a few bands in Pb−30%Bi alloy are shown in Figs. 5(a) and (b), respectively. Composition measurements for Pb−26%Bi and Pb−30%Bi alloys by EPMA are presented in Figs. 5(c) and (d), respectively. For the $\alpha\rightarrow\beta$ transition boundary, the α phase has an average composition of approximately 24.0% Bi and the β phase is close to 30.1% Bi. According to Fig. 5(d), an average composition of the α phase is about 26.3% Bi, and the composition of β phase is about 32.3% Bi. It can be seen that the composition increases in α bands and decreases in β bands and there is a step change in either the $\alpha\rightarrow\beta$ or $\beta\rightarrow\alpha$ phase transition boundary. Table 2 lists the compositions of β phase at all the transition boundaries for the banding structure.

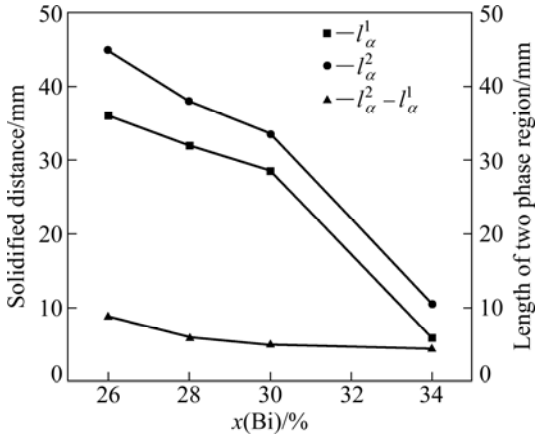

Fig. 4 Variation of solidification distances for formation of β phase, end of α phase and length of two phase region with different alloy compositions

Table 2 Measured compositions of banding structures

Banding Ⅰ	Banding Ⅱ	Banding Ⅲ
$\alpha\rightarrow\beta$, $\beta\rightarrow\alpha$	$\alpha\rightarrow\beta$, $\beta\rightarrow\alpha$	$\alpha\rightarrow\beta$
33.5%Bi, 28.7%Bi	33.6%Bi, 28.1%Bi	34.3%Bi

3.4 Nucleation undercoolings of α and β phases

From the composition measurements at the boundaries of the bands, the nucleation undercooling for α and β phases can be determined by using the phase diagram. According to the results obtained from LIU and TRIVEDI [16], the compositions at which the transitions occur should not be influenced by the growth conditions, such as diffusive or convective growth.

Table 2 shows that the average composition of the solid β phase at the $\alpha\rightarrow\beta$ transition boundary layer is 33.8% Bi. This composition corresponds to the nucleation temperature of 172.5 °C, which is 14.5 °C below the peritectic temperature, as shown by point A in Fig. 6. At this temperature, the extrapolated α phase liquidus composition is 42.1% Bi, as shown by point B. The β liquidus temperature at 42.1% Bi is 177 °C, as shown by point C, so that the undercooling for the β phase to nucleate is obtained as Δt_n^β =4.5 °C.

The α phase nucleation temperature can be evaluated similarly by using the composition of the β phase at the $\beta\rightarrow\alpha$ transition boundary layer. This composition ($c_{\beta/\alpha}^\beta$) is measured to be 28.4% Bi as listed

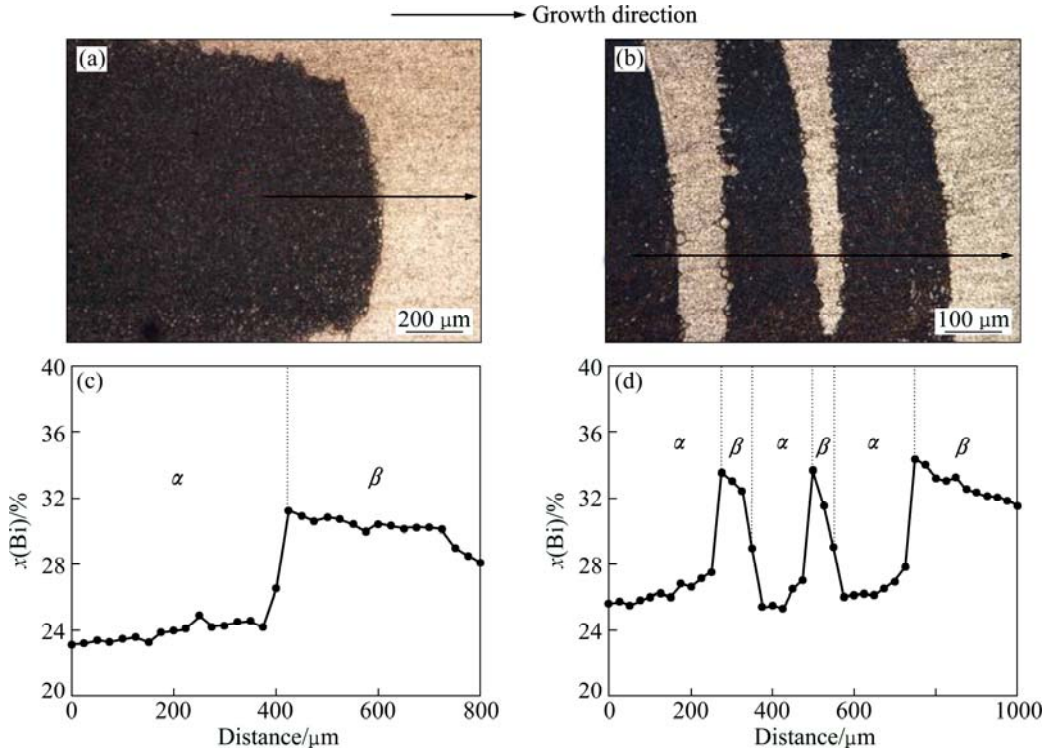

Fig. 5 OM images and concentration distribution measured by EMPA: (a, c) Pb−26%Bi; (b, d) Pb−30%Bi

in Table 2, as shown by point *D* in Fig. 6. Therefore, *α* phase nucleation occurs at the interface temperature of 194 °C where the *β* liquidus composition is obtained 35% Bi, as shown by point *E*. The *α* phase liquidus temperature at 35% Bi is 203 °C, as shown by point *F*, so that the undercooling for the *α* phase to nucleate is obtained as Δt_n^{α}=9 °C, as shown in Fig. 6.

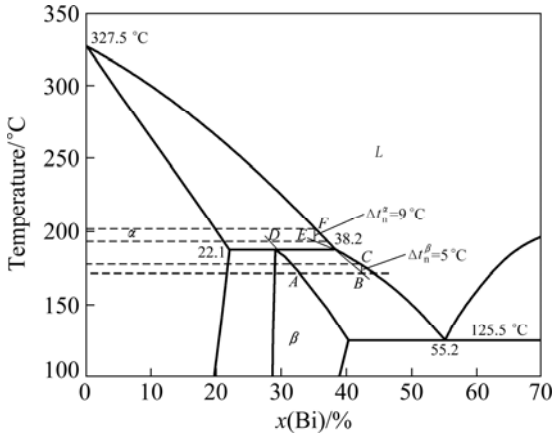

Fig. 6 Nucleation undercooling of *α* and *β* phases in banding structure of Pb−Bi alloys

3.5 Banding window for banding structure

According to the boundary layer model developed by KARMA et al [17], the banding window for a semi-infinite sample can be obtained by using theoretical calculation. The minimum value $c_0^{\min}$ and maximum value $c_0^{\max}$ of the banding window can be calculated by the following equations:

$$c_0^{\min}=[k_\alpha+\exp(-\Delta)\times(1-k_\alpha)](c_L+\frac{\Delta t_n^{\beta}}{m_\beta-m_\alpha}) \quad (1)$$

$$c_0^{\max}=[k_\beta+\exp(-\Delta)\times(1-k_\beta)](c_L-\frac{\Delta t_n^{\alpha}}{m_\beta-m_\alpha}) \quad (2)$$

where Δ is the convection parameter and defined as:

$$\Delta=\frac{d}{l_p} \quad (3)$$

where d is the boundary layer thickness; l_p is the steady-state diffusion length, $l_p=D/v_p$; D is the diffusion coefficient and v_p is the pulling velocity. In the present study, v_p is equal to the growth rate of solid/liquid interface v because of the low solidification rate. In the purely diffusive regime, d is far larger than l_p, therefore, $\Delta\to\infty$. Equations (1) and (2) can be written as:

$$c_0^{\min}=k_\alpha(c_L+\frac{\Delta t_n^{\beta}}{m_\beta-m_\alpha}) \quad (4)$$

$$c_0^{\max}=k_\beta(c_L-\frac{\Delta t_n^{\alpha}}{m_\beta-m_\alpha}) \quad (5)$$

While in the convective regime, the minimum and maximum compositions of the banding window are related to Δ. The relationships among $c_0^{\min}$, $c_0^{\max}$ and Δ are calculated by substituting the parameters (Table 3)

into Eqs. (1) and (2), respectively, as shown in Fig. 7. Where the white region corresponds to $\Delta t_n^{\alpha} = \Delta t_n^{\beta}$ =2 °C and the gray shaded region corresponds to Δt_n^{α} =9 °C and Δt_n^{β} =4.5 °C. It is clearly seen that the values of both $c_0^{\min}$ and $c_0^{\max}$ increase with decreasing convection parameter (Δ), and the composition range becomes narrower with smaller Δ, which means convection would narrow the composition range.

In the present study, the transient banding structure is observed for all the studied Pb−Bi alloys. It indicates that the $c_0^{\max}$ should be larger than 34%, or equal to 34% at least. Thus it is obviously seen that the composition range with Δt_n^{α} =9 °C and Δt_n^{β} =4.5 °C does not agree with the present experimental results. Then the calculated undercoolings of α and β phases are not correct based on the composition of β phase in the Section 3.4. That may be contributed from the fluctuation of nucleation temperatures which result in the variation of undercooling to nucleation. On the contrary,

Table 3 Physical parameters of Pb−Bi alloy [16,17]

Symbol	Parameter	Value	Unit
t_p	Peritectic temperature	187	°C
c_α	Composition (Bi) of α at t_p	22.1	%
c_β	Composition (Bi) of β at t_p	29.2	%
c_L	Composition (Bi) of L at t_p	38.2	%
m_α	α-liquidus slope	−5.01	°C/%
m_β	β-liquidus slope	−2.17	°C/%
k_α	Distribution coefficient of α	0.579	
k_β	Distribution coefficient of β	0.764	
Γ	Gibbs-Thomson coefficient	1.3×10^{-7}	m·K
D	Diffusion coefficient in liquid	1.3×10^{-5}	cm^2/s

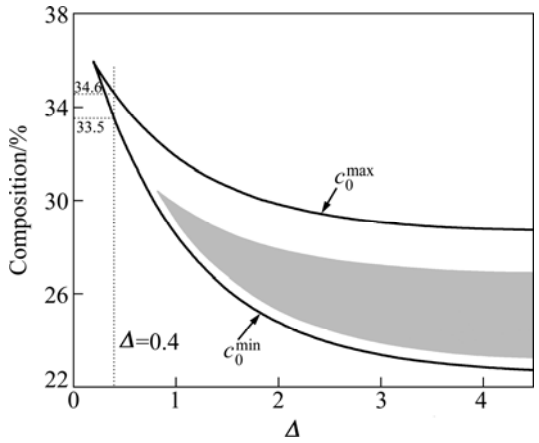

Fig. 7 Variation of composition range of banding structures with convection parameter for Pb−Bi alloys (White region corresponds to $\Delta t_n^{\alpha} = \Delta t_n^{\beta}$ =2 °C and gray shaded region corresponds to Δt_n^{α} =9 °C and Δt_n^{β} =4.5 °C)

the assumption of both Δt_n^{α} and Δt_n^{β} equal to 2 °C is appropriate.

LIU and TRIVEDI [16] assumed that the convection parameter Δ=0.8 for samples of 0.4 mm in diameter is in a good agreement between their theoretical calculations and experimental results. In the present study, the sample diameter is 1.8 mm, thus the convection is stronger than that in sample of 0.4 mm in diameter. Therefore, Δ is assumed to be 0.4 in the present study. The $c_0^{\min}$ and $c_0^{\max}$ can be calculated by using Eqs. (1) and (2), and they are 33.5% and 34.6%, respectively. This composition range is in accordance with the experimental results in the present study.

3.6 Initial α phase formation and macrosegregation

During the growth of initial primary α phase, the solute concentration of the α/liquid interface c_L^{α} varies with solidification distance z_S, and the relationship between c_L^{α} and z_S can be obtained by using the boundary layer model developed by KARMA et al [17]. c_L^{α} can also be presented as a function of melt composition c_m:

$$c_L^{\alpha} = k_e^{\alpha} c_m / k_{\alpha} \tag{6}$$

where k_e^{α} is the effective distribution coefficient of α phase, given as:

$$k_e^{\alpha} = \frac{k_{\alpha}}{k_{\alpha} + \exp(-\Delta)(1-k_{\alpha})} \tag{7}$$

where k_α is the distribution coefficient of α.

The equation of motion for $dc_m(t)/dt$ is obtained as follows:

$$\frac{dc_m(t)}{dt} = \frac{v(t)[c_m(t) - k_{\alpha} c_L^{\alpha}(t)]}{l_S - z_S(t)} \tag{8}$$

The growth velocity of α-liquid interface v is given as:

$$v(t) = \frac{dz_S}{dt} \tag{9}$$

Combining Eqs. (6), (8) and (9), it is obtained

$$\frac{dc_m}{c_m - k_e^{\alpha} c_m} = \frac{dz_S}{l_S - z_S} \tag{10}$$

Integrating the both sides of Eq. (10) from 0 to z_S, which yields

$$\int_{c_0}^{c_m} \frac{1}{c_m - k_e^{\alpha} c_m} dc_m = \int_0^{z_S} \frac{1}{l_S - z_S} dz_S \tag{11}$$

$$\frac{1}{1-k_e^{\alpha}} \ln c_m \Big|_{c_0}^{c_m} = -\ln(l_S - z_S)\Big|_0^{z_S} \tag{12}$$

where c_0 is the composition of the alloy.

Finally, the equation for c_m is derived as:

$$c_m = c_0(1-f_\alpha)^{(k_e^\alpha-1)} \tag{13}$$

where f_α is the volume fraction of initial α phase, defined as $f_\alpha = z_S / l_S$. The relationship between c_m and z_S can be calculated by combining Eqs. (7) and (13). The results are shown in Fig. 8. It is clearly seen that c_m increases with increasing solidification distance. The shaded strip is the banding window which is obtained by using Eqs. (1) and (2) with $\Delta t_n^\alpha = \Delta t_n^\beta$ =2 °C. The minimum composition (c_0^{min}) and maximum composition (c_0^{max}) of the banding window are 33.5% Bi and 34.6% Bi, respectively. In a finite sample, c_m is a monotonously increasing function of time (or position along the sample) because of the excess solute buildup in the mixed liquid zone outside the diffusion boundary layer, as reflected by the trajectory of c_m in Fig. 8. In this case, banding only occurs in the section of the sample where the trajectory of c_m traverses the shaded strip, that is, when c_m traverses the composition range, banding would occur. This is clearly seen in Fig. 8, where banding occurs when c_m crosses this strip for 26%, 28%, 30% and 34% Bi alloys, which agrees well with the experimental results.

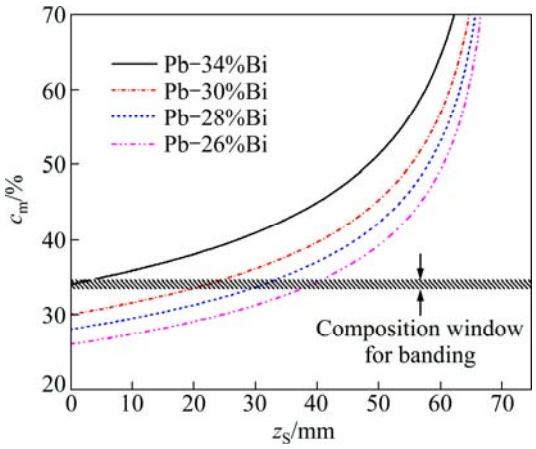

Fig. 8 Relationship between c_m and z_S (Shaded strip corresponds to composition range for banding structures)

Then, equations (6), (7) and (13) are used to obtain the relationship between c_L^α and z_S, as shown in Fig. 9. It is clearly seen that c_L^α increases with increasing solidification distance, which means the solute would pile up in front of the solid/liquid interface. Therefore, an enrichment of solute at the solid/liquid interface would occur.

$$c_L^\alpha = \frac{c_0 k_e^\alpha (1-\frac{z_S}{l_S})^{k_e^\alpha-1}}{k_\alpha} \tag{14}$$

The solute concentration of solid phase c_S can be calculated by using Eqs. (7) and (14). The relationship between c_S and z_S is shown in Fig. 10. It indicates that the c_S for all the alloys increases with increasing solidification distance. It implies that a macrosegregation would be observed during the growth of α phase, and it results from the melt convection as:

$$c_S = c_L^\alpha k_\alpha = c_0 k_e^\alpha (1-\frac{z_S}{l_S})^{k_e^\alpha-1} \tag{15}$$

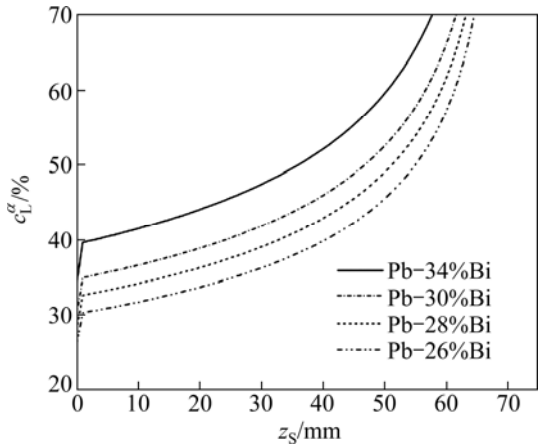

Fig. 9 Relationship between c_L^α and z_S

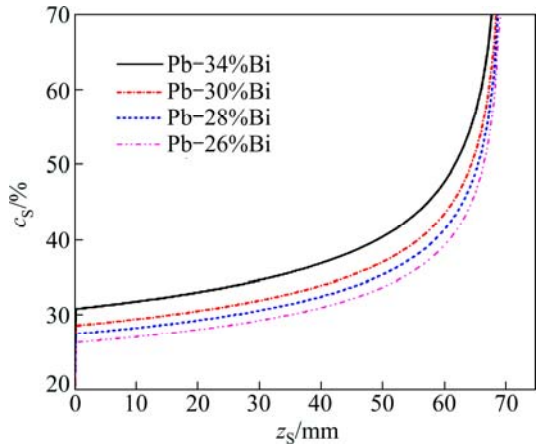

Fig. 10 Relationship between c_S and z_S

The temperature of the α/liquid interface is equal to the nucleation temperature of β phase, namely, $t_i^\alpha = t_n^\beta$ as the concentration of α/liquid interface (c_L^α) increases to a critical value. Therefore, the β phase would nucleate at the S/L interface of α phase. While, t_i^α and t_n^β can be written as:

$$t_i^\alpha = t_m^\alpha + c_L^\alpha m_\alpha \tag{16}$$

$$t_n^\beta = t_m^\beta + m_\beta c_L^\alpha - \Delta t_n^\beta \tag{17}$$

It is obtained by equating these two temperatures

$$c_L^\alpha = \frac{t_m^\alpha - t_m^\beta + \Delta t_n^\beta}{m_\beta - m_\alpha} = c_L + \frac{\Delta t_n^\beta}{m_\beta - m_\alpha} \tag{18}$$

Combining Eq. (18) with Eq. (14), it is obtained

$$\frac{c_0 k_e^\alpha (1-\frac{z_S^1}{l_S})^{k_e^\alpha-1}}{k_\alpha} = c_L + \frac{\Delta t_n^\beta}{m_\beta - m_\alpha} \tag{19}$$

where

$$\frac{z_S^1}{l_S} = f_\alpha^1 \tag{20}$$

is the solidified fraction of initial primary α phase before the nucleation of peritectic β phase at the S/L interface, and it is listed in Table 1. Taking logarithm on both sides of Eq. (19), it is obtained

$$\ln(1-f_\alpha^1) = \frac{\ln\left[(c_L + \frac{\Delta t_n^\beta}{m_\beta - m_\alpha})k_\alpha / k_e^\alpha\right] - \ln c_0}{k_e^\alpha - 1} \tag{21}$$

The relationship between $\ln(1-f_\alpha^1)$ and $\ln c_0$ can be obtained by substituting the parameters of the Pb−Bi system (Table 3) into Eq. (21). The calculated results are shown in Fig. 11. Compared with the experimental results (Table 1), a good agreement is achieved.

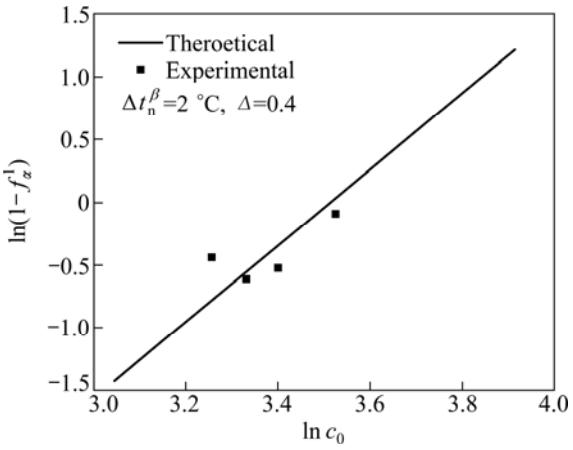

Fig. 11 Plots of $\ln(1-f_\alpha^1)$ vs $\ln c_0$ for experimental data in Table 1 and theoretical model

4 Conclusions

1) The banding structures are observed in both hypoperitectic and hyperperitectic compositions of Pb−Bi alloys. The bands do not form continuously but the band formation is destabilized by convection after a few bands are formed. Additionally, the widths of the α and β bands do not remain constant, but the α phase width decreases with distance and ultimately vanishes so that only the β phase continues to form.

2) The banding composition range is calculated by using the Karma's model, and it becomes narrower with increasing strength of convection. Comparing the calculated results with the experimental results, it is found that the assumption of both Δt_n^α and Δt_n^β equal to 2 °C, and Δ equal to 0.4 is appropriate.

3) In a finite sample, melt composition is a monotonously increasing function of time (or position along the sample) because of the excess solute buildup in the mixed liquid zone outside the diffusion boundary layer. Banding only occurs in the section of the sample when c_m traverses the composition range, where banding would occur.

4) Macrosegregation should be observed during the initial α phase formation, and the solidified fraction of initial α phase decreases with increasing composition of Bi.

References

[1] SU Y Q, LUO L S, LI X Z, GUO J J, YANG H M, FU H Z. Well-aligned in situ composites in directionally solidified Fe−Ni peritectic systems [J]. Applied Physics Letters, 2006, 89: 231918-1−3.

[2] LO T S, DOBLER S, PLAPP M, KARMA A, KURZ W. Two-phase microstructure selection in peritectic solidification: From island banding to coupled growth [J]. Acta Materialia, 2003, 51: 599−611.

[3] VANDYOUSSEFI M, KERR H W, KURZ W. Two-phase growth in peritectic Fe−Ni alloys [J]. Acta Materialia, 2000, 48: 2297−2306.

[4] SUMIDA M. Evolution of two phase microstructure in peritectic Fe–Ni alloy [J]. Journal of Alloys and Compounds, 2003, 349: 302−310.

[5] LEE J H, VERHOEVEN J D. Peritectic formation in the Ni−Al system [J]. Journal of Crystal Growth, 1994, 144: 353−366.

[6] TRIVEDI R. Theory of layered-structure formation in peritectic systems [J]. Metallurgical and Materials Transactions A, 1995, 26: 1583−1590.

[7] BOETTINGER W J. The structure of directionally solidified two-phase Sn−Cd peritectic alloys [J]. Metallurgical Transactions, 1974, 5: 2023−2031.

[8] YASUDA H, NOTAKE N, TOKIEDA K, OHNAKA I. Periodic structure during unidirectional solidification for peritectic Cd−Sn alloys [J]. Journal of Crystal Growth, 2000, 210: 637−645.

[9] TRIVEDI R, PARK J S. Dynamics of microstructure formation in the two-phase region of peritectic systems [J]. Journal of Crystal Growth, 2002, 235: 572−588.

[10] PARK J S, TRIVEDI R. Convection-induced novel oscillating microstructure formation in peritectic systems [J]. Journal of Crystal Growth, 1998, 187: 511−515.

[11] TITCHENER A P, SPITTLE J A. The microstructures of directionally solidified alloys that undergo a peritectic transformation [J]. Acta Metallurgica, 1975, 23: 497−502.

[12] TOKIEDA K, YASUDA H, OHNAKA I. Formation of banded structure in Pb−Bi peritectic alloys [J]. Materials Science and Engineering A, 1999, 262: 238−245.

[13] LOGRASSO T A, FUH B C, TRIVEDI R. Phase selection during directional solidification of peritectic alloy [J]. Metallurgical and Materials Transactions A, 2005, 36: 1287−1300.

[14] HU X W, LI S M, CHEN W J, GAO S F, LIU L, FU H Z. Primary dendrite arm spacing during unidirectional solidification of Pb–Bi peritectic alloys [J]. Journal of Alloys and Compounds, 2009, 484: 631−636.

[15] HU X W, LI S M, GAO S F, LIU L, FU H Z. Peritectic

transformation and primary dendrite dissolution in directionally solidified Pb–26%Bi alloy [J]. Journal of Alloys and Compounds, 2010, 501: 110−114.

[16] LIU S, TRIVEDI R. Effect of thermosolutal convection on microstructure formation in the Pb−Bi peritectic system [J]. Metallurgical and Materials Transactions A, 2006, 37: 3293−3304.

[17] KAEMA A, RAPPEL W J, FUH B C, TRIVEDI R. Model of banding in diffusive and convective regimes during directional solidification of peritectic systems [J]. Metallurgical and Materials Transactions A, 1998, 29: 1457−1470.

Pb−Bi 包晶合金定向凝固过程中带状组织的形成

胡小武[1]，李双明[2]，艾凡荣[1]，闫 洪[1]

1. 南昌大学 机电工程学院，南昌 330031

2. 西北工业大学 凝固技术国家重点实验室，西安 710072

摘 要：采用 Bridgman 定向凝固技术对 Pb−Bi 包晶合金进行定向凝固实验，生长速度为 0.5 μm/s，温度梯度为 35 K/mm。在亚包晶和过包晶成分的 Pb−Bi 合金中(Pb−*x*Bi，*x*=26%，28%，30%和 34%)均观察到带状组织。由于熔体对流的影响，在试样中心形成树状初生 α 相，周围被包晶 β 相基体包围。带状组织出现在树状组织后，并且该带状组织为过渡性的。测定带状组织中的成分分布，从而确定 α 和 β 两相的形核过冷度。在有限长试样中，熔体对流是形成过渡性带状组织的主要原因，该过渡性带状组织表现为有限带数，带宽不恒定，且在 Pb−Bi 合金的两相包晶区很宽的成分范围内出现。

关键词：定向凝固；偏析；Bridgman 技术；Pb−Bi 合金；带状组织

(Edited by FANG Jing-hua)